NRG Oncology Updated International Consensus Atlas on Pelvic Lymph Node Volumes for Intact and Post-Operative Prostate Cancer

William A. Hall, MD[1], Eric Paulson, PhD[1], Brian J. Davis, MD, PhD[2], Daniel E. Spratt, MD[3], Todd M. Morgan, MD[4], David Dearnaley, FRCR[5], Alison C Tree, MD[5], Jason A. Efstathiou, MD, DPhil[6], Mukesh Harisinghani, MD[7], Ashesh B. Jani, MD, MSEE[8], Mark K Buyyounouski, MD, MS[9], Thomas M Pisansky, MD[2], Phuoc T. Tran, MD, PhD[10], R. Jeffrey Karnes[11], MD, Ronald C. Chen, MD, MPH, FASCO[12], Fabio L. Cury, MD[13], Jeff M. Michalski, MD, MBA, FASTRO[14], Seth A. Rosenthal, MD, FACR, FASTRO[15], Bridget F. Koontz, MD[16], Anthony C. Wong, MD, PhD[17], Paul Nguyen, MD[18], Thomas A. Hope, MD[19], Felix Feng, MD[17], Howard M Sandler, MD, FASCO, FASTRO[20], Colleen AF Lawton, MD, FACR, FASTRO[1]

1- Medical College of Wisconsin, Department of Radiation Oncology
2- Mayo Clinic, Department of Radiation Oncology
3- University of Michigan, Department of Radiation Oncology
4- University of Michigan, Department of Urology
5- The Royal Marsden NHS Foundation Trust and The Institute of Cancer Research, London, UK
6- Massachusetts General Hospital, Department of Radiation Oncology
7- Massachusetts General Hospital, Department of Radiology
8- Emory University, Department of Radiation Oncology
9- Stanford University, Department of Radiation Oncology
10- Johns Hopkins, Department of Radiation Oncology
11- Mayo Clinic, Department of Urology
12- University of Kansas, Department of Radiation Oncology
13- McGill University, Department of Radiation Oncology
14- Washington University, Department of Radiation Oncology
15- Sutter Medical Group, Department of Radiation Oncology
16- Duke Cancer Institute, Department of Radiation Oncology
17- University of California San Francisco, Department of Radiation Oncology
18- Dana Farber Harvard Cancer Center, Department of Radiation Oncology
19- University of California San Francisco, Department of Radiology
20- Cedars-Sinai Medical Center, Department of Radiation Oncology

Acknowledgements: Medical College of Wisconsin Libraries, MIM technical support (MIM Inc, Beachwood, OH), Katie Kruger for meeting coordination and manuscript formatting, National Institute for Health Research (NIHR) Biomedical Research Centre at The Royal Marsden NHS Foundation Trust and the Institute of Cancer Research, London, and the Michigan Radiation Oncology Quality Consortium (MROQC) for community review and feedback.

Running Title: NRG Oncology Pelvic Nodal Contouring Atlas

Corresponding Author: William A. Hall, MD, whall@mcw.edu, 8701 W Watertown Plank Rd, Milwaukee, WI 53226, phone- 414-805-4477, fax- 414-805-4369, statistical analyses: Eric Paulson, PhD, 414-805-447, 8701 W Watertown Plank Rd, Milwaukee, WI 53226

Funding: No specific funding was allocated for this project

Data Sharing: "Research data are stored in an institutional repository and will be shared upon request to the corresponding author."

Disclosures: Dr. Ronald Chen reports personal fees from Abbvie, personal fees from Accuray, outside the submitted work; Dr. Cury reports grants and non-financial support from Boston Scientific, personal fees from Varian Medical Systems, grants from Sanofi, outside the submitted work; Dr. Davis reports personal fees from Boston Scientific, Inc., outside the submitted work; Dr. Dearnaley reports personal fees from The Institute of Cancer Research, during the conduct of the study; In addition, Dr. Dearnaley has a patent EP1933709B1 issued. Dr. Efstathiou reports personal fees from Blue Earth Diagnostics, personal fees from Boston Scientific, personal fees from AstraZeneca, personal fees from Taris Biomedical, personal fees from Janssen, personal fees from Bayer Healthcare, personal fees from Roivant Pharma, outside the submitted work; Dr. Feng reports personal fees from Dendreon, personal fees from EMD Serono, personal fees from Janssen Oncology, personal fees from Ferring, personal fees from Sanofi, personal fees from Bayer, personal fees from Blue Earth Diagnostics, personal fees from Celgene, personal fees from Medivation/Astellas, personal fees from Clovis Oncology, other from PFS Genomics, personal fees from Genentech, other from Nutcracker Therapeutics, outside the submitted work; In addition, Dr. Feng has a patent EP3047037 A4 issued. Dr. Hall reports technical support from MIM Software Inc, during the conduct of the study; other from Elekta AB, outside the submitted work. Dr. Hope reports grants from Philips Healthcare, grants from Advanced Accelerator Applications, personal fees from Curium, personal fees from Ipsen, outside the submitted work; Dr. Koontz reports grants from Janssen Scientific Affairs, grants and personal fees from Blue Earth Diagnostics, grants from Merck, personal fees from Demos Publishing, outside the submitted work; Dr. Nguyen reports personal fees from COTA, grants and personal fees from Astellas, grants and personal fees from Bayer, grants and personal fees from Janssen, personal fees from Ferring, personal fees from Astellas, personal fees and other from Augmenix, personal fees from Dendreon, personal fees from Blue Earth DIagnostics, personal fees from Boston Scientific, outside the submitted work; Dr. Paulson reports other from Elekta AB, outside the submitted work. Dr. Sandler reports personal fees from Janssen, other from Radiogel, outside the submitted work; and Member, ASTRO Board of Directors. Dr. Spratt reports personal fees from Janssen, personal fees from Blue Earth, from AstraZenica, outside the submitted work; Dr. Tran reports grants from Astellas Pharm, grants from Bayer Healthcare, grants, personal fees and other from RefleXion Medical Inc, personal fees from Noxopharm, outside the submitted work; In addition, Dr. Tran has a patent Compounds and Methods of Use in Ablative Radiotherapy. Patient#: 9114158. licensed to Natsar Pharm. Dr. Tree reports grants and personal fees from Elekta, grants from Accuray, grants from Varian, personal fees from Janssen, non-financial support from Astellas, personal fees from Genesis healthcare, personal fees from Ferring, outside the submitted work; All other authors have nothing to disclose.

Abstract:

Purpose/Objectives:

In 2009, the Radiation Therapy Oncology Group (RTOG) genitourinary (GU) members published a consensus atlas for contouring prostate pelvic nodal clinical target volumes (CTV). Data has emerged further informing nodal recurrence patterns. The objective of this study is to provide an updated prostate pelvic nodal consensus atlas.

Materials/Methods:

A literature review was performed abstracting data on nodal recurrence patterns. Data was presented to a panel of international experts, including radiation oncologists, radiologists, and urologists. After data review, participants contoured nodal CTVs on three cases: post-operative, intact node positive, and intact node negative. Radiation oncologist contours were analyzed qualitatively using count maps which provided a visual assessment of controversial regions and quantitatively analyzed using Sorensen-Dice similarity coefficients, and Hausdorff distances compared with the 2009 RTOG atlas. Diagnostic radiologists generated a reference table outlining considerations for determining clinical node positivity.

Results:

Eighteen radiation oncologists' contours (54 CTVs) were included. Two urologists' volumes were examined in a separate analysis. The mean CTV for the post-op case was 302 cc, intact node

positive case was 409 cc, and intact node negative case 342 cc. Compared to the original RTOG consensus, the mean Sorensen-Dice similarity coefficient for the post-op case was 0.63 (SD 0.13), intact node positive case was 0.68 (SD 0.13), and intact node negative case 0.66 (SD 0.18). The mean Hausdorff Distance (in cm) for the post-op case was 0.24 (SD 0.13), the intact node positive case was 0.23 (SD 0.09), and intact node negative case 0.33 (SD 0.24). Four regions of CTV controversy were identified and consensus for each of these areas was reached.

Conclusions:

Discordance with the 2009 RTOG consensus atlas was seen in a group of experienced NRG Oncology and international GU radiation oncologists. To address areas of variability and account for new data, an updated NRG Oncology consensus contour atlas was developed.

45

46

47 **Introduction:**

48 The treatment of pelvic lymph nodes with external beam radiation therapy (RT) is a frequent
49 component of the management of patients with prostate cancer[1]. Pelvic lymph node irradiation
50 is a common practice for men receiving prostate RT with high-risk disease, clinically lymph
51 node-positive disease, as well as in the post-prostatectomy setting[2-4]. There exists a wide range
52 of approaches to pelvic nodal contouring and identification of pelvic nodal regions considered
53 to be "at risk." Treated volumes have also been historically correlated with clinical outcomes for
54 prostate patients[5]. The Radiation Therapy Oncology Group (RTOG) developed a consensus-
55 based contouring atlas in 2009 that has served as a foundation for nodal contouring on several
56 prospective clinical trials[6]. This guideline has also been used in standard clinical practice. A
57 consensus atlas encourages a consistent application of nodal treatments across providers and
58 institutions to allow further understanding of the effects of this component of treatment.

59

60 Since publication of the original RTOG atlas, additional patterns of tumor recurrence data have
61 emerged through both retrospective and prospective imaging studies. Multiple publications
62 have presented data to support a change in recommendations for pelvic nodal contouring from
63 the original RTOG consensus atlas[7-11]. Given these data, the NRG Oncology Genitourinary (GU)
64 core committee thought it was appropriate to update the consensus atlas for pelvic nodal
65 contouring, and expand the existing atlas to address the post-operative and clinically node-

positive settings. The objective of this study was to both expand and refine the existing consensus nodal atlas to account for contemporary research findings.

Methods:

The first and senior authors (***) along with the NRG Oncology GU core committee recruited an international panel of physicians including radiation oncologists, diagnostic radiologists (with expertise in nuclear medicine and magnetic resonance imaging (MRI)), and urologists. The study was IRB approved by the *** Institutional Review Board (***) prior to initiating research activities. All participants in the contouring effort were informed via email correspondence and verbal review at the start of the video conferencing of their rights as participants in this nodal contouring effort. Care was taken to anonymize individual observer contour contributions within the group.

The first step in the update was a literature review on pelvic nodal recurrence patterns published since 2007. This literature search was performed in collaboration with the *** Libraries. Primary search sources included: 1) PubMed (((pelvic AND (lymph node drainage OR lymphatic drainage))) AND prostate cancer) and 2) Google Scholar (terms: prostate cancer nodal drainage, prostate cancer nodal radiation, prostate cancer nodal failure patterns, post-operative prostate cancer nodal failure, prostate-specific membrane antigen (PSMA) nodal failure, fluciclovine F-18 nodal failure patterns, and C-11 Choline PET prostate lymph nodes. Along with the above primary search terms, several additional “similar publication” links from the above references were used. Finally, all participants were asked to

send relevant literature and references to the first author (***) for review, organization, and presentation. Publications selected by the group were considered representative of the most recent and relevant data in four different categories: 1) existing updated nodal consensus atlases, 2) modern surgical/intact disease lymphatic drainage patterns, 3) post-operative recurrence patterns and 4) novel molecular positron emission tomography (PET) based recurrence patterns. Publications were presented in detail via video conferencing for discussion and commentary from all members in the group. Figures were reviewed with the group, including locations of failure patterns. Surgeons and radiologists participated in these calls and were available for commentary and questions. Following the video conferencing presentations, slides (with notes from the video conferencing) were then circulated to all participants for further individual review.

Following this data presentation, radiation oncologists were asked to contour the nodal clinical target volume (CTV). A total of three cases formed the primary contouring subjects. These cases were selected by the first and senior authors (*** and ***). Case 1 was a 58-year-old male with history of unfavorable intermediate risk adenocarcinoma of the prostate, clinical stage T1cN0M0, Grade group 3, Gleason score 4+3, initial serum prostate specific antigen (PSA) of 5.92 ng/mL, who underwent surgical resection. Final pathology showed Grade group 3, Gleason score 4+3 adenocarcinoma, positive margins, extensive seminal vesicle involvement, along with 1/8 nodes positive in a right obturator node (pT3bN1M0). Case 2 was a 66-year-old male with high risk adenocarcinoma of the prostate who underwent a biopsy due to a PSA rising to 13.7 ng/mL. Biopsy showed, Grade group 4, Gleason score 4+4, with clinical stage of T2bN1M0. He was clinically node positive, with two enlarged regional nodes on his diagnostic pelvic

110 computed tomography (CT). Case 3 was a 65 y/o male with high risk adenocarcinoma of the
111 prostate, clinical stage T2aN0M0, Grade group 5, Gleason score 4+5, PSA 38.2 ng/mL.

112 Urologists (*** and ***) were also asked to contour "dissection" regions using their anticipated
113 dissection templates using Case 3. These surgical contours were not included in the primary
114 nodal contouring analysis. Contours were completed using MIM cloud (MIM Software Inc,
115 Ohio). Contouring physician observers were blinded to other participants' contour results
116 during this process of contouring. Only the first, second, and senior author (***, ***, and ***)
117 had access to all contour results collectively. Observers were required to contour a nodal
118 clinical target volume (CTV), and if so inclined, also to contour a nodal gross tumor volume
119 (GTV).
120 Contour analysis was performed using Sorensen-Dice similarity coefficient and Hausdorff
121 distance[12,13]. These metrics were calculated and compared to a baseline contour that was
122 created by the first (***) and senior (***) authors following the 2009 RTOG nodal contouring
123 atlas[6]. The contour volumes were statistically compared using a Mann-Whitney test. The CTV
124 contours of all individual observers were used to create a count map having the same
125 resolution as the underlying image modality. Within such a count map, each voxel value is
126 determined by the superposition of observers that included the corresponding image voxel
127 within their CTV. For 18 observers, the maximum count is 18. If all image voxels were included
128 in a contour, they would present as a solid single color. If some of the voxels were not included
129 in a contour set, they would present as a different color, based on the number of observers that
130 included those voxels. Within a count map, different iso-surfaces with different colors were
131 created. A total of 18 colors would be available with 18 observers. This enabled very careful

132 “qualitative” observation of specific regions that were controversial, and presented a method
133 to highlight specific areas of controversy for focused discussion and arbitration. The spread in
134 volume over these percentile surfaces provided an indication of the CTV similarities within the
135 observers and also highlighted controversial regions. This method also provided a means by
136 which to visually highlight particular areas of disagreement that were present in contoured
137 volumes amongst the observers. Diagnostic radiologists (XX and XX) presented a summary of
138 criteria for node positivity in the pelvis using a variety of imaging modalities. (Table 1)
139
140 Results of the consensus contouring exercise were subsequently reviewed at the January 2020
141 NRG Oncology meeting in person for those attending and were simultaneously presented via
142 video conferencing for those unavailable to attend. Finally areas of controversy identified in the
143 contour analytics were adjudicated via an anonymous online survey. The new step-by-step
144 contour recommendations were reviewed and circulated to the group. Common dose and
145 fractionation schedules and corresponding constraints were included for group review and
146 comment. Community radiation oncology feedback on these updates was solicited from the
147 Michigan Radiation Oncology Quality Consortium (MROQC) via video conference and email.
148
149 **Results:**
150 Eighteen radiation oncologists finished three full contour sets for a total of 54 volumes, all of
151 which were included in the final contour analysis. The urologists’ contours were not included in
152 the final consensus contour analysis but instead were used for observation and consideration

153 only. Observers practiced in the United States, Canada, and the United Kingdom with a median
154 of more than 15 years of practice.
155
156 The mean CTV for the post-op case was 302 cubic centimeters (cc), intact node positive case
157 was 409 cc, and intact node negative case 342 cc. As compared with the original RTOG
158 consensus atlas contour (created by authors *** and ***) the mean Sorensen-Dice similarity
159 coefficient for the post-op case was 0.63 (SD 0.13), intact node positive case was 0.68 (SD 0.13),
160 and intact node negative case 0.66 (SD 0.18). The mean Hausdorff Distance (in cm) for the post-
161 op case was 0.24 (SD 0.13), the intact node positive case was 0.23 (SD 0.09), and intact node
162 negative case 0.33 (SD 0.24). These values represented the "quantitative" contour results.
163
164 Several "qualitative" variations were identified when using the count maps. Taken collectively,
165 these variations provided a visual representation of consensus ("warmer" colors, e.g. yellow,
166 green) and controversial ("cooler" colors, e.g. magenta) areas. The four areas of greatest
167 variability consisted of: 1) the superior most aspect of the common iliac nodes, 2) the transition
168 from the external iliac to the inguinal nodes, 3) the inclusion of the peri-prostatic nodes, and 4)
169 the inclusion of peri-rectal nodes (**Figure 1a-1d**). Contours of clinically positive nodes were also
170 controversial. These areas were discussed in detail via in person meeting and video
171 conferencing, and were also the subject of specific questions in the anonymous survey. The
172 results of the survey formed the consensus steps (1-10) below. Consensus on final borders for
173 each of these areas was reached via written survey specifically addressing potential changes to
174 these areas. The refined steps to contour the nodal CTV can be seen below.

175

176 *Prophylactic nodal contouring steps for clinically node negative patients including both intact*

177 *and post-op cases:* ***Figure 2a-m and Figure 3a-g***

178

179 1. *Commence contours at the bifurcation of the aorta into the common iliac arteries or the*

180 *proximal inferior vena cava to the common iliac veins, whichever occurs more superiorly*

181 *(typically at the level of L4-L5). (Figure 2a-b)*

182 2. *Contour approximately 5-7 mm around each iliac vessel, including the entire*

183 *circumference of both the iliac artery and vein. Bone, bowel, bladder, and muscle should*

184 *be excluded from the nodal CTV contour. Where clinically indicated, CTV margins can be*

185 *more generous, particularly anterior to vessels (10 mm). Ensure coverage posteriorly in*

186 *the area formed between the psoas major and the vertebral body. (Figure 2c-d)*

187 3. *The width of the inter-space between the external and internal iliac contours should be*

188 *approximately 1.5-3 cm. This will vary depending on patient anatomy. (Figure 2e)*

189 4. *Include the pre-vertebral, pre-sacral, and posterior mesorectal nodes to the bottom of*

190 *S3. (Figure 2f)*

191 5. *The posterior border of the CTV coming off the internal iliac vessels should extend to the*

192 *anterior edge of the piriformis muscle following the course of the pudendal artery and*

193 *inferior gluteal artery. (Figure 2g-h)*

194 6. *The transition from the external iliac to the inguinal nodes occurs when the external iliac*

195 *vessels cross beneath the inguinal ligament into the inguinal canal. Examine for this*

196 *transition, and begin tapering off external iliac nodes at that point. This should*

correspond to the entrance of the vascular structures into the inguinal canal (Figure 2i), often best seen on the coronal images. (Figure 2j)

7. *The external iliac contours should typically end when the vessels are completely lateral to the most medial aspect of the acetabulum (near mid femoral head and fovea). At that point, the contours should be tapered off. (Figure 2k-l)*
8. *The obturator nodes can be between 1-2 cm in width, and should extend to the posterior edge of the obturator internus muscle. (Figure 2k)*
9. *Begin to taper the obturator nodes at the top of the seminal vesicles (or the top of the post-op bed), extending approximately 1 cm anterior to the anterior edge of the obturator internus muscle. (Figure 2k-l) (MRI registration can be useful in this area)*
10. *The obturator nodes should end where the seminal vesicles join the prostate, or approximately the midportion of the contoured post op CTV bed. (Figure 2m)*

Modifications when treating clinically node positive cases:

1. *Steps 1-10 should be followed above for prophylactic regions.*
2. *Table 1 should be referenced to help identify suspicious nodes, all suspicious nodes should be considered for review with diagnostic radiology and contoured as appropriate.*
3. *Prophylactic nodal volumes should extend approximately 5-7 mm around clinically suspicious nodes, this may alter the prophylactic nodal volumes in step 1-10.*
4. *Residual (shrunken) gross nodes, post androgen deprivation therapy (ADT), should form the primary boost volume (additional information in dosing section below).*

Radiation dosing to pelvic nodes:

- *<u>Prophylactic Nodes:</u> A dose range of 45-50.4 Gy is acceptable when using conventional fractionation. The majority of participants do not change their prophylactic nodal dose whether treating an intact prostate case or postoperative.*
- *<u>Gross nodes:</u> Should be treated as high as clinically feasible (up to the dose being delivered to the primary tumor) while respecting normal organ tolerances. Nodal volumes should be examined pre and post-ADT, and the post ADT tumor volume should serve as the high dose boost volume.*

Overarching points for consideration when contouring pelvic nodes with the new guidelines:

- *All available/relevant scans (such as PET and MR) should be carefully considered by the radiation oncologist when delineating nodal coverage.*
- *In general, the CTV should exclude bone, bladder, muscle, and bowel*
- *Simulation images that are suggestive of clinically suspicious nodes (criteria in Table 1) should be reviewed with a diagnostic radiologist and may be included in boost volumes at the clinical discretion of the radiation oncologist.*
- *In some circumstances, small portions of bowel may abut vascular structures or large portions of small bowel may be in the pelvis. As mentioned above (step 2) the CTV should exclude bowel (including both small and large bowel). Rarely, bowel may be included in the CTV at the discretion of the radiation oncologist secondary to extenuating clinical circumstances (eg. adjacent involved node or tumor extension). Normal tissue constraints should be prioritized by the radiation oncologist when*

240 *treating pelvic nodes. Clinical review and discretion on the part of the radiation*
241 *oncologist is needed in each of these circumstances.*
242 • *For postoperative cases: pathology and operative reports should be carefully considered*
243 *in treatment volumes. Regions with pathologically involved nodes that exhibit*
244 *extranodal tumor extension may have more generous CTVs. Surgical clips should be*
245 *identified and potentially included at the discretion of the radiation oncologist. Close*
246 *collaboration with colleagues having expertise in Urology and Diagnostic Radiology is*
247 *recommended. Altered lymph node spread is common[14], and larger volume expansions,*
248 *including post-operative changes of uncertain significance may also be necessary. PET*
249 *scans or other advanced imaging acquired should be registered and included in the*
250 *treatment planning process.*
251 • *Consideration should be given to the comorbidities and medical history of each*
252 *individual patient*
253
254 The results of areas that urologic surgeons identified as part of their dissection template are
255 presented in **Supplemental Figure 1**. Finally, given the wide range of contour volumes, an
256 example of a larger contour set, including peri-rectal nodes, can be seen in **Supplemental**
257 **Figure 2**. Such expanded volumes may be rarely considered for highly select and advanced T4
258 lesions at the discretion of the radiation oncologist[15]. Considerable discretion is needed when
259 including mesorectal nodes in the treatment volume, and normal tissue constraints should be
260 prioritized.
261

262 **Table 1** was created by the diagnostic radiologists (***, ***) and nuclear medicine expert (***)
263 to include criteria for clinical node positive prostate lesions[16-21]. These criteria are helpful for
264 radiation oncologists to be aware of and most importantly discuss with their diagnostic
265 radiology and nuclear medicine colleagues. In addition, commonly used dose constraints were
266 collated for different dose and fractionation schedules and are displayed in **Table 2a-c**[22-25]**.**
267 These may be helpful for radiation oncologists to consider when treating pelvic nodes.
268
269 **Discussion:**
270 Prophylactic treatment of pelvic lymph nodes in the management of prostate cancer remains
271 an active area of clinical inquiry and investigation which presently lacks consensus. Data is
272 emerging suggesting some efficacy to pelvic nodal treatment[1]. In the context of this ongoing
273 inquiry, expert consensus-based guidelines consider its use an acceptable management
274 option[3,4]. Constant evaluation and evidence-based updating of available consensus guidelines
275 are imperative. Careful examination of the evolution of guidelines over time is essential to
276 ensure evidence based improvement. The overarching goal of our process was to perform a
277 timely evaluation and update the 2009 RTOG consensus guidelines. We did not seek to reinvent
278 the atlas, rather sought to update and refine it.
279
280 Our study shows the 2009 RTOG pelvic lymph node consensus guidelines no longer accurately
281 reflect the practice patterns of prostate cancer experts from around the world, nor adequately
282 reflect the state-of-the art assessment of lymph node regions at risk for prostate cancer
283 metastasis. Furthermore, we developed a guideline process to develop treatment volume

contouring standards that could be used as a template for other disease sites, and for research or clinical collaboratives.

These guidelines were updated using an evidence-based process. There were several categories of updated data that were considered in detail by the group of observers that participated in this contouring effort. These publications fell into four broad categories: 1) existing updates to contouring guidelines, 2) surgical mapping and lymphatic drainage series, 3) clinical recurrence series, and 4) PET/post-operative recurrence series. There have been a few proposed modifications by international groups to the existing RTOG nodal contouring atlas that were considered in detail by the authors. The first was an updated atlas produced by the PIVOTAL Trialists group[8], of which one author (***) also participated as an international representative in this NRG Oncology contouring activity. The PIVOTAL atlas recommended modifications to the existing RTOG contouring recommendations but did not include node positive, PET, MRI or post-operative nodal contouring recommendations. The second recently updated consensus atlas that specifically focused on prostate nodal treatment was from the Groupe d'Etude des Tumeurs Uro-Génitales (GETUG)[7]. This atlas incorporated some novel PET recurrence pattern data available at that time. The GETUG atlas does not include specific contouring recommendations for node positive or post-operative patients. The NRG Oncology group provides the current updated consensus atlas with three overarching goals: 1) refining the current RTOG intact prophylactic atlas recommendations, 2) addressing clinically node positive disease, 3) addressing contouring in the post-operative setting.

306 The second broad category of data considered was newly available surgical data. Much of this
307 focused on novel sentinel node data and other surgical nodal mapping techniques. Current
308 surgical methods of addressing pelvic nodes were considered. Most contemporary surgical
309 guidelines recommend an extended pelvic lymph node dissection when a nodal dissection is
310 performed.[4,26,27] Surgical dissection and nodal mapping data provided valuable insight into
311 common sites of nodal drainage. This data partially informed the updated nodal atlas
312 recommendations. It is notable that internal iliac, external iliac, and obturator nodes comprise
313 the vast majority of nodal drainage sites of the prostate. However, the common iliac, pre-sacral,
314 and paraaortic/caval nodes can also represent 10% or more of nodal drainage sites
315 mapped.[26,28-31] Other drainage sites, such as perirectal nodes, have also represented over 10%
316 of nodal drainage sites in some sentinel node mapping series, but this is highly variable and
317 inconsistent[31]. Appropriate applications of this data were considered carefully by the panel, it
318 should be noted that inclusion of these more generous nodal volumes should be highly
319 selected.
320
321 The third general category of data that was considered included novel MRI techniques and
322 newly published clinical patterns of recurrence data. Several series directly compared the
323 anatomical distribution of nodal metastases with the published RTOG contouring guideline.
324 Meijer et al. examined MR lymphography in a modern cohort of intact intermediate and high
325 risk patients and noted that over fifty percent of patients had positive nodes outside of the
326 RTOG nodal atlas contoured volumes. Common sites were in the high common iliac, perirectal,
327 and para-aortic regions[9]. It was also noted that a high percentage of patients in the post-

328 operative setting had aberrant nodal spread, with a particularly large percentage of patients
329 exhibiting nodal spread in the perirectal area.[14] Patterns of recurrence data have also been
330 published directly comparing failure patterns to the existing RTOG atlas. Spratt et al. conducted
331 a retrospective series of pelvic nodal failures and mapped those in relation to the existing RTOG
332 nodal atlas[10]. This series concluded that an increase in the superior border of the pelvic nodal
333 treatment volume to cover the common iliac stations to L4/L5 would cover over 90% of first
334 nodal recurrences[10]. Such findings regarding the common iliac nodal stations have been
335 supported by other publications, demonstrating that a number of recurrences were located
336 outside of the standard RTOG atlas treatment volumes.[32,33]
337
338 The final category of contemporary data considered was novel prostate-specific PET data. More
339 specifically how prostate PET scans might influence nodal volumes in both the intact treatment
340 naïve setting and the post-operative, biochemically recurrent setting. Series including PSMA,
341 Fluciclovine F18, and C-11 choline PET were considered and reviewed. Several of the published
342 PSMA PET series mapped areas of nodal recurrence that were outside of the existing RTOG
343 template. These recurrence locations were presented and reviewed by the observers for
344 consideration as to how this might influence the existing nodal treatment volumes[11,34-38].
345 Several of these series visually mapped PET recurrence locations in relation to the existing
346 RTOG consensus atlas[39].
347
348 Following the literature review, a comprehensive contouring exercise took place. There were
349 both quantitative and qualitative assessments of these contour results. The quantitative results

350 of the contouring exercise yielded Sorensen-Dice coefficients reflecting poor agreement.[40]
351 These findings were consistent within the post-operative contours, intact node positive, and
352 intact node negative contour sets. Qualitatively, there were a total of four areas that were
353 visually identified as controversial using the count map strategy. The count map strategy was
354 felt to be very helpful to recognize areas needing focused discussion as compared with just the
355 numerical metrics. Considered collectively, these metrics were supportive of the need for an
356 updated consensus contouring atlas. There are several areas of this updated atlas that differ
357 from the existing 2009 RTOG atlas. Areas that differ include the superior, vascular margins, and
358 inferior boundary recommendations.
359
360 There are a few important points to be considered when examining the new contouring steps
361 presented. These are intended to provide approximate guidelines, but not rigidly constrain the
362 radiation oncologist from exercising clinical judgement in an individual case. Radiation
363 oncologists should carefully examine and incorporate all oncologic and diagnostic scan
364 information into their treatment plans. There are clinical circumstances that may warrant more
365 generous treatment volumes, or more constrained treatment volumes. Factors specific to the
366 comorbidities and individual patient medical history should also be considered. We have
367 presented variations for consideration, along with step-by- step guidelines to ensure an
368 overarching consensus recommendation.
369
370 As novel PET-based imaging continues to develop, this additional information may help
371 individualize RT planning. There are many published series highlighting apparently atypical

anatomical sites of nodal recurrence, such as in peri-rectal or peri-aortic nodes[39]. Particularly peri-rectal nodes were a source of significant discussion, particularly for T4 tumors[15]. Routinely including areas such as the peri-rectal region, was thought by the majority of the group to create an unnecessarily large treatment volume. However, a variation in contours is also presented for consideration (Supplemental Figure 2) when considered clinically indicated by the radiation oncologist. Other studies have recently addressed considerably more generous treatment volumes and the tolerance of such an approach[41]. As mentioned, advanced molecular imaging studies should be reviewed by radiation oncologists, in collaboration with nuclear medicine, whenever available.

There are limitations to this activity that merit consideration. We do not address the controversial topic of “indications” for pelvic nodal RT. That is currently the subject of multiple trials, (NCT01368588, NCT01952223, ISRCTN80146950) and is considered beyond the scope of the current study. This study does not aggregate or meta-analyze formally all reported PET based patterns of failure, this was also considered beyond the scope of the current study. We also did not address the ideal planning target volume definition. This will depend on target proximity to organs-at-risk and image-guidance methods. This is a consensus atlas that went through extensive revision, refinement, and peer review, prospective validation of the atlas was not formally conducted. Dosimetric constraints are presented for consideration, however optimal dose constraints was not the primary focus of the analysis, these should be interpreted accordingly. Finally, we acknowledge that any guideline is a “work-in-progress”, and that refinement and enhancement is expected as the science that forms its basis advances.

The objective and results of this study serve as a refinement and evidence-based update to the existing RTOG atlas. Our aspiration was to account for recently published PET and MRI based nodal recurrence data, which supports a prudent expansion of target volumes. In addition, we have presented higher resolution CT and MRI sets, with annotations that may assist in education and obtaining uniformity of practice. Full DICOM image files, with contoured structure sets, can be made available as supplements in order to provide greater detail for practitioners.

Conclusions:

A new NRG Oncology consensus nodal contouring atlas is presented, with several changes to the existing RTOG consensus atlas. Extensive imaging data and studies provided a basis for the CTV volumes that radiation oncologists should consider when targeting pelvic nodal tissues. The included guidelines are intended to provide greater detail and account for recently published nodal failure pattern data. Moreover, variations in contouring strategies are presented, along with dosimetric constraints for consideration when treating the pelvic lymph nodes.

416 **REFERENCES:**

417 1. Pollack A, Karrison T, Balogh JA, Low D, Bruner D. Short Term Androgen Deprivation
418 Therapy Without or With Pelvic Lymph Node Treatment Added to Prostate Bed Only
419 Salvage Radiotherapy: The NRG Oncology/RTOG 0534 SPPORT Trial. *Int J Radiat Oncol*
420 *Biol Phys.* 2018;102(5):1605.

421 2. Lieng H, Kneebone A, Hayden AJ, et al. Radiotherapy for node-positive prostate cancer:
422 2019 Recommendations of the Australian and New Zealand Radiation Oncology Genito-
423 Urinary group. *Radiother Oncol.* 2019;140:68-75.

424 3. Heidenreich A, Bastian PJ, Bellmunt J, et al. EAU guidelines on prostate cancer. part 1:
425 screening, diagnosis, and local treatment with curative intent-update 2013. *Eur Urol.*
426 2014;65(1):124-137.

427 4. Mohler JL, Antonarakis ES, Armstrong AJ, et al. Prostate Cancer, Version 2.2019, NCCN
428 Clinical Practice Guidelines in Oncology. *J Natl Compr Canc Netw.* 2019;17(5):479-505.

429 5. Roach M, 3rd, DeSilvio M, Valicenti R, et al. Whole-pelvis, "mini-pelvis," or prostate-only
430 external beam radiotherapy after neoadjuvant and concurrent hormonal therapy in
431 patients treated in the Radiation Therapy Oncology Group 9413 trial. *Int J Radiat Oncol*
432 *Biol Phys.* 2006;66(3):647-653.

433 6. Lawton CA, Michalski J, El-Naqa I, et al. RTOG GU Radiation oncology specialists reach
434 consensus on pelvic lymph node volumes for high-risk prostate cancer. *Int J Radiat*
435 *Oncol Biol Phys.* 2009;74(2):383-387.

436 7. Sargos P, Guerif S, Latorzeff I, et al. Definition of lymph node areas for radiotherapy of
437 prostate cancer: A critical literature review by the French Genito-Urinary Group and the
438 French Association of Urology (GETUG-AFU). *Cancer Treat Rev.* 2015;41(10):814-820.
439 8. Harris VA, Staffurth J, Naismith O, et al. Consensus Guidelines and Contouring Atlas for
440 Pelvic Node Delineation in Prostate and Pelvic Node Intensity Modulated Radiation
441 Therapy. *Int J Radiat Oncol Biol Phys.* 2015;92(4):874-883.
442 9. Meijer HJ, Fortuin AS, van Lin EN, et al. Geographical distribution of lymph node
443 metastases on MR lymphography in prostate cancer patients. *Radiother Oncol.*
444 2013;106(1):59-63.
445 10. Spratt DE, Vargas HA, Zumsteg ZS, et al. Patterns of Lymph Node Failure after Dose-
446 escalated Radiotherapy: Implications for Extended Pelvic Lymph Node Coverage. *Eur*
447 *Urol.* 2017;71(1):37-43.
448 11. Schiller K, Devecka M, Maurer T, et al. Impact of (68)Ga-PSMA-PET imaging on target
449 volume definition and guidelines in radiation oncology - a patterns of failure analysis in
450 patients with primary diagnosis of prostate cancer. *Radiat Oncol.* 2018;13(1):36.
451 12. Taha AA, Hanbury A. An efficient algorithm for calculating the exact Hausdorff distance.
452 *IEEE Trans Pattern Anal Mach Intell.* 2015;37(11):2153-2163.
453 13. Sorensen-Dice. MathWorks. https://www.mathworks.com/help/images/ref/dice.html.
454 Published 2019. Accessed.
455 14. Meijer HJ, van Lin EN, Debats OA, et al. High occurrence of aberrant lymph node spread
456 on magnetic resonance lymphography in prostate cancer patients with a biochemical

457 recurrence after radical prostatectomy. *Int J Radiat Oncol Biol Phys.* 2012;82(4):1405-
458 1410.
459 15. Abu-Gheida I, Bathala TK, Maldonado JA, et al. Increased frequency of Mesorectal and
460 Perirectal LN involvement in T4 Prostate Cancers. *Int J Radiat Oncol Biol Phys.* 2020.
461 16. Ramirez M, Ingrand P, Richer JP, et al. What is the pelvic lymph node normal size?
462 Determination from normal MRI examinations. *Surg Radiol Anat.* 2016;38(4):425-431.
463 17. Maurer T, Eiber M, Schwaiger M, Gschwend JE. Current use of PSMA-PET in prostate
464 cancer management. *Nat Rev Urol.* 2016;13(4):226-235.
465 18. Hofman MS, Lawrentschuk N, Francis RJ, et al. Prostate-specific membrane antigen PET-
466 CT in patients with high-risk prostate cancer before curative-intent surgery or
467 radiotherapy (proPSMA): a prospective, randomised, multi-centre study. *Lancet.*
468 2020;395(10231).
469 19. Songmen S, Nepal P, Olsavsky T, Sapire J. Axumin Positron Emission Tomography: Novel
470 Agent for Prostate Cancer Biochemical Recurrence. *J Clin Imaging Sci.* 2019;9:49.
471 20. Eiber M, Herrmann K, Calais J, et al. Prostate Cancer Molecular Imaging Standardized
472 Evaluation (PROMISE): Proposed miTNM Classification for the Interpretation of PSMA-
473 Ligand PET/CT. *J Nucl Med.* 2018;59(3):469-478.
474 21. Savir-Baruch B, Banks KP, McConathy JE, et al. ACR-ACNM Practice Parameter for the
475 Performance of Fluorine-18 Fluciclovine-PET/CT for Recurrent Prostate Cancer. *Clin Nucl*
476 *Med.* 2018;43(12):909-917.

477 22. Wilkins A, Naismith O, Brand D, et al. Derivation of Dose/Volume Constraints for the
478 Anorectum from Clinician- and Patient-Reported Outcomes in the CHHiP Trial of
479 Radiation Therapy Fractionation. *Int J Radiat Oncol Biol Phys.* 2020;106(5):928-938.
480 23. Ferreira MR, Thomas K, Truelove L, et al. Dosimetry and Gastrointestinal Toxicity
481 Relationships in a Phase II Trial of Pelvic Lymph Node Radiotherapy in Advanced
482 Localised Prostate Cancer. *Clin Oncol (R Coll Radiol).* 2019;31(6):374-384.
483 24. Michalski JM, Gay H, Jackson A, Tucker SL, Deasy JO. Radiation dose-volume effects in
484 radiation-induced rectal injury. *Int J Radiat Oncol Biol Phys.* 2010;76(3 Suppl):S123-129.
485 25. Murray J, Gulliford S, Griffin C, et al. Evaluation of erectile potency and radiation dose to
486 the penile bulb using image guided radiotherapy in the CHHiP trial. *Clin Transl Radiat*
487 *Oncol.* 2020;21:77-84.
488 26. Mattei A, Fuechsel FG, Bhatta Dhar N, et al. The template of the primary lymphatic
489 landing sites of the prostate should be revisited: results of a multimodality mapping
490 study. *Eur Urol.* 2008;53(1):118-125.
491 27. Mottet N, Bellmunt J, Bolla M, et al. EAU-ESTRO-SIOG Guidelines on Prostate Cancer.
492 Part 1: Screening, Diagnosis, and Local Treatment with Curative Intent. *Eur Urol.*
493 2017;71(4):618-629.
494 28. de Korne CM, Wit EM, de Jong J, et al. Anatomical localization of radiocolloid tracer
495 deposition affects outcome of sentinel node procedures in prostate cancer. *Eur J Nucl*
496 *Med Mol Imaging.* 2019;46(12):2558-2568.

497 29. Harke NN, Godes M, Wagner C, et al. Fluorescence-supported lymphography and
498 extended pelvic lymph node dissection in robot-assisted radical prostatectomy: a
499 prospective, randomized trial. *World J Urol.* 2018;36(11):1817-1823.
500 30. Nguyen DP, Huber PM, Metzger TA, Genitsch V, Schudel HH, Thalmann GN. A Specific
501 Mapping Study Using Fluorescence Sentinel Lymph Node Detection in Patients with
502 Intermediate- and High-risk Prostate Cancer Undergoing Extended Pelvic Lymph Node
503 Dissection. *Eur Urol.* 2016;70(5):734-737.
504 31. Winter A, Kowald T, Paulo TS, et al. Magnetic resonance sentinel lymph node imaging
505 and magnetometer-guided intraoperative detection in prostate cancer using
506 superparamagnetic iron oxide nanoparticles. *Int J Nanomedicine.* 2018;13:6689-6698.
507 32. De Bruycker A, De Bleser E, Decaestecker K, et al. Nodal Oligorecurrent Prostate Cancer:
508 Anatomic Pattern of Possible Treatment Failure in Relation to Elective Surgical and
509 Radiotherapy Treatment Templates. *Eur Urol.* 2019;75(5):826-833.
510 33. Parker WP, Evans JD, Stish BJ, et al. Patterns of Recurrence After Postprostatectomy
511 Fossa Radiation Therapy Identified by C-11 Choline Positron Emission
512 Tomography/Computed Tomography. *Int J Radiat Oncol Biol Phys.* 2017;97(3):526-535.
513 34. Schiller K, Sauter K, Dewes S, et al. Patterns of failure after radical prostatectomy in
514 prostate cancer - implications for radiation therapy planning after (68)Ga-PSMA-PET
515 imaging. *Eur J Nucl Med Mol Imaging.* 2017;44(10):1656-1662.
516 35. Calais J, Kishan AU, Cao M, et al. Potential Impact of (68)Ga-PSMA-11 PET/CT on the
517 Planning of Definitive Radiation Therapy for Prostate Cancer. *J Nucl Med.*
518 2018;59(11):1714-1721.

519 36. Habl G, Sauter K, Schiller K, et al. (68) Ga-PSMA-PET for radiation treatment planning in
520 prostate cancer recurrences after surgery: Individualized medicine or new standard in
521 salvage treatment. *Prostate.* 2017;77(8):920-927.
522 37. Byrne K, Eade T, Kneebone A, et al. Delineating sites of failure following post-
523 prostatectomy radiation treatment using (68)Ga-PSMA-PET. *Radiother Oncol.*
524 2018;126(2):244-248.
525 38. Sinha S, Witztum A, Vasudevan H, et al. 68Ga-PSMA-11 PET-Based Prostate Cancer
526 Lymph Node Atlas Reveals Patterns of Potential Geographic Miss in Consensus Pelvic
527 Nodal Contours. *Int J Radiat Oncol Biol Phys.* 2019;105(1):S136.
528 39. Schiller K, Stöhrer L, Düsberg M, et al. PSMA-PET/CT-based Lymph Node Atlas for
529 Prostate Cancer Patients Recurring After Primary Treatment: Clinical Implications for
530 Salvage Radiation Therapy. *Eur Urol Oncol.* 2020.
531 40. Delpon G, Escande A, Ruef T, et al. Comparison of Automated Atlas-Based Segmentation
532 Software for Postoperative Prostate Cancer Radiotherapy. *Front Oncol.* 2016;6:178.
533 41. Jethwa KR, Hellekson CD, Evans JD, et al. (11)C-Choline PET Guided Salvage Radiation
534 Therapy for Isolated Pelvic and Paraortic Nodal Recurrence of Prostate Cancer After
535 Radical Prostatectomy: Rationale and Early Genitourinary or Gastrointestinal Toxicities.
536 *Adv Radiat Oncol.* 2019;4(4):659-667.
537
538
539
540

FIGURE CAPTIONS:

Figure 1: Count Maps Showing Controversial Regions Identified

Figure 2 (A-M): New Consensus Contours on CT

Figure 3 (A-G): New Consensus Contours on MR

Supplemental Figure 1: Surgical Contours Representing Areas for Dissection

Supplemental Figure 2: Contours including some Peri-rectal and lower pre-sacral nodal regions

Table 2: Constraints for consideration when treating pelvic nodes:

Table 2a: 75.6-79.2 Gy in 42-44 fractions, treating nodes to 45-50.4 Gy with a sequential boost	
Rectum (24)	V (≥ 4500 cGy) ≤ 50%
	V (≥ 7000 cGy) ≤ 15%
	V (> 7200 cGy) < 10 cc
Bladder	V (≥ 4500 cGy) ≤ 50%
	V (≥ 7000 cGy) ≤ 15%
Femur_L	V (≥ 5000 cGy) ≤ 2%
	Dmax ≤ 5250 cGy
Femur_R	V (≥ 5000 cGy) ≤ 2%
	Dmax ≤ 5250 cGy
Colon	V (≥ 6000 cGy) ≤ 2%
	Dmax ≤ 6250 cGy
Small Bowel (bowel loops)	V (≥ 5000 cGy) ≤ 10%
	Dmax ≤ 5200 cGy
Pubic Bone	V (≥ 7000 cGy) ≤ 25%
Penile Bulb (should not sacrifice PTV coverage)	V (≥ 5000 cGy) ≤ 50%
Table 2b: 70 Gy in 28 fractions, treating nodes to 45-50.4 Gy with a simultaneous integrated boost	
Rectum (24)	V (≥ 4500 cGy) ≤ 45%
	V (≥ 5500 cGy) ≤ 25%
	V (≥ 6500 cGy) ≤ 15%
	V (> 6500 cGy) < 10 cc
Bladder	V (≥ 4500 cGy) ≤ 45%
	V (≥ 5500 cGy) ≤ 25%
	V (≥ 6500 cGy) ≤ 15%
Femur_L	V (≥ 5000 cGy) ≤ 1%
	Dmax ≤ 5250 cGy
Femur_R	V (≥ 5000 cGy) ≤ 1%
	Dmax ≤ 5250 cGy
Colon	Dmax ≤ 5500 cGy
Small Bowel (bowel loops)	V (≥ 4650 cGy) ≤ 2 cc
	Dmax ≤ 5200 cGy
Pubic Bone	V (≥ 6000 cGy) ≤ 30%
Penile Bulb (should not sacrifice PTV coverage)	Make dose as low as reasonably achievable
Table 2c: 60 Gy in 20 fractions (treating nodes to 44-47 Gy over 20 fractions*) (8)	
Rectum (22)	V (≥ 2000 cGy) ≤ 85% (no circumferential dose)
	V (≥ 3000 cGy) ≤ 57%
	V (≥ 4000 cGy) ≤ 38%
	V (≥ 5000 cGy) ≤ 22%
	V (≥ 6000 cGy) ≤ 1%
Bladder**	V (≥ 4000 cGy) ≤ 50%
	V (≥ 4800 cGy) ≤ 25%
	V (≥ 5680 cGy) ≤ 5%
	V (≥ 6000 cGy) ≤ 3 %
Femur_L	V (≥ 3500 cGy) ≤ 5%
	Dmax ≤ 3700 cGy

	Dmax ≤ 3700 cGy
Colon	Dmax ≤ 5000 cGy
Small Bowel (bowel loops)	Dmax ≤ 4000 cGy
	V (≥ 3700 cGy) ≤ 90 cc
	V (≥ 3300 cGy) ≤ 130 cc
Pubic Bone	V (≥ 5700 cGy) ≤ 20%
Penile Bulb (25)	V (≥ 2200 cGy) ≤ 50%

*Safety and efficacy of hypofractionation to pelvic nodes is currently the subject of ongoing investigation and has not been established

**Patient reported quality of life data for the bladder constraints is the subject of ongoing investigation

Anatomic Location	CT/MRI-based Size	CT/MRI-based Morphology	PSMA PET-based Criteria	Axumin PET-based Criteria	Example of positive node on CT	Example of positive node on MR	Example of positive node on PET
Mesorectal, Presacral	Short axis > 4 mm	Irregular Border and/or heterogenous morphology (only for LN > 3mm on MRI)	Uptake greater than blood pool	> 1 cm: Uptake greater than BM < 1 cm: Uptake greater than blood pool	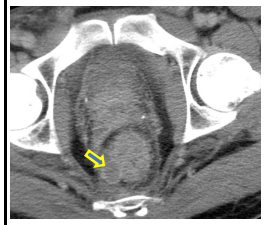	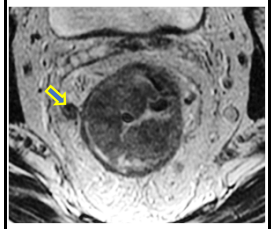	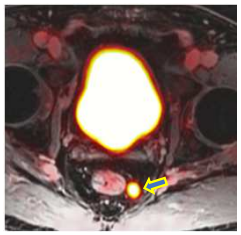
Internal Iliac, Obturator	Short axis > 7mm	Irregular Border and/or heterogenous morphology	Uptake greater than blood pool	> 1 cm: Uptake greater than BM < 1 cm: Uptake greater than blood pool	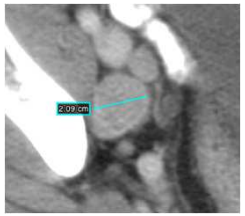	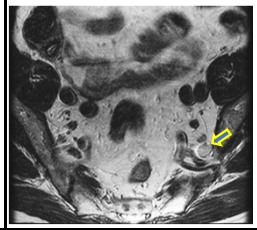	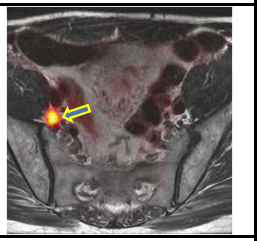
Common Iliac and External Iliac	Short axis > 8 mm	Irregular Border and/or heterogenous morphology	Uptake greater than blood pool	> 1 cm: Uptake greater than BM < 1 cm: Uptake greater than blood pool	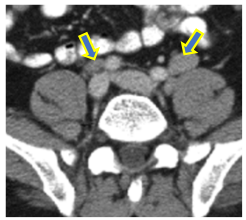	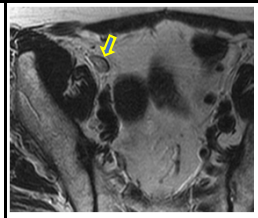	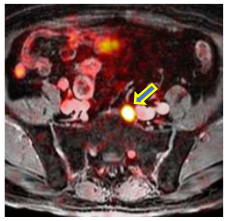
Inguinal	Short axis > 8 mm	Irregular Border and/or heterogenous morphology	Asymmetric uptake that is greater than liver	Asymmetric uptake greater than BM	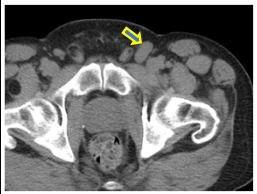	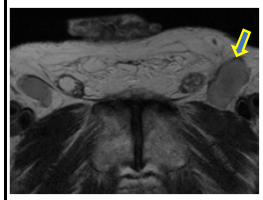	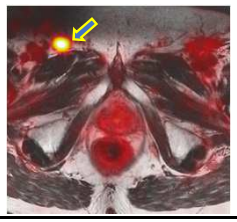

Anatomic Location	CT/MRI-based Size	CT/MRI-based Morphology	PSMA PET-based Criteria	Axumin PET-based Criteria	Example of positive node on CT	Example of positive node on MR	Example of positive node on PET
Mesorectal, Presacral	Short axis > 4 mm	Irregular Border and/or heterogenous morphology (only for LN > 3mm on MRI)	Uptake greater than blood pool	> 1 cm: Uptake greater than BM < 1 cm: Uptake greater than blood pool	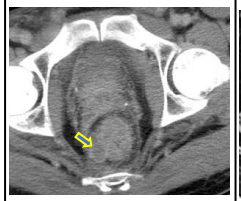	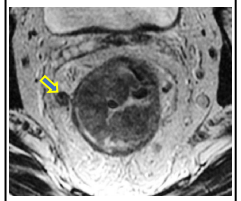	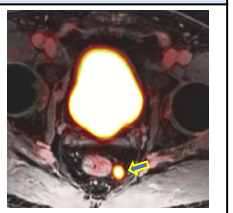
Internal Iliac, Obturator	Short axis > 7mm	Irregular Border and/or heterogenous morphology	Uptake greater than blood pool	> 1 cm: Uptake greater than BM < 1 cm: Uptake greater than blood pool	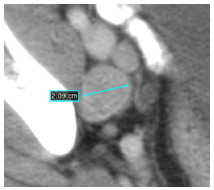	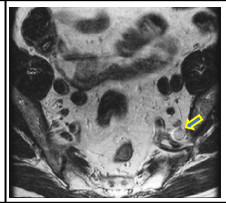	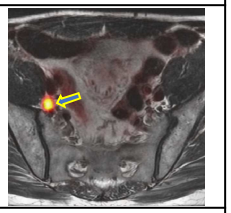
Common Iliac and External Iliac	Short axis > 8 mm	Irregular Border and/or heterogenous morphology	Uptake greater than blood pool	> 1 cm: Uptake greater than BM < 1 cm: Uptake greater than blood pool	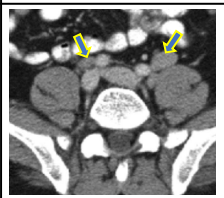	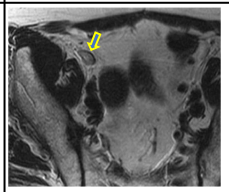	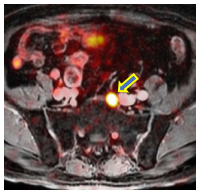
Inguinal	Short axis > 8 mm	Irregular Border and/or heterogenous morphology	Asymmetric uptake that is greater than liver	Asymmetric uptake greater than BM	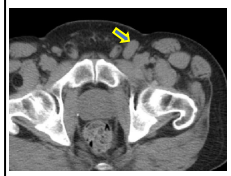	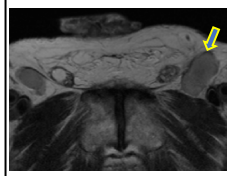	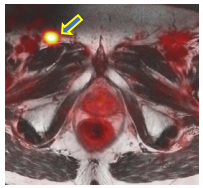

Figure 1:

Figure 1a:

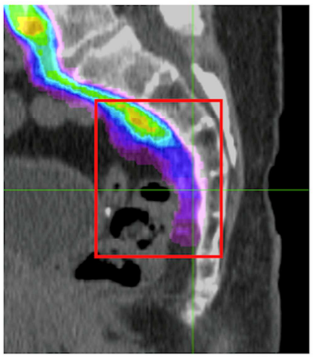

Figure 1b:

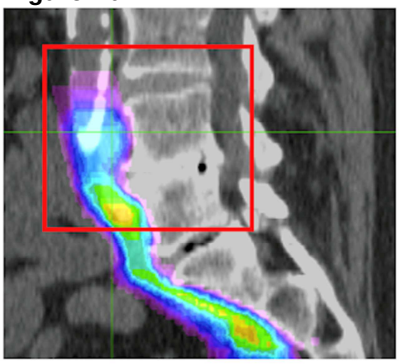

Figure 1c:

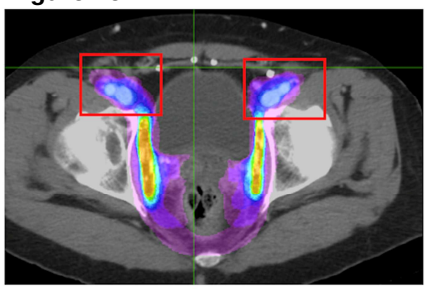

Figure 1d:

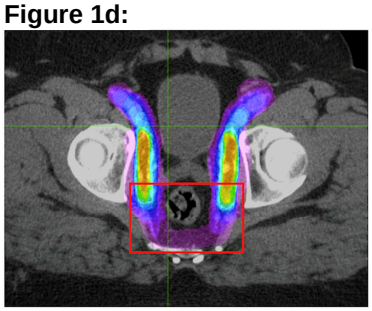

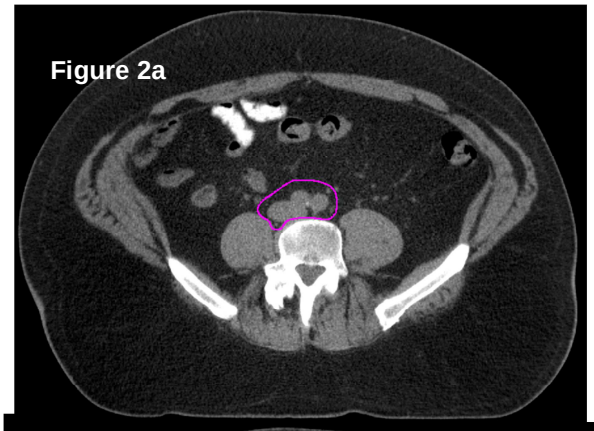
Figure 2a

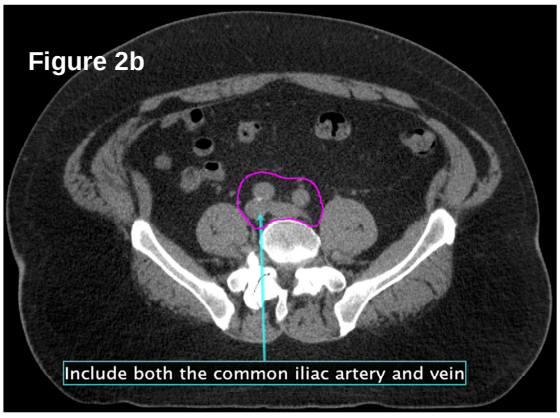
Figure 2b
Include both the common iliac artery and vein

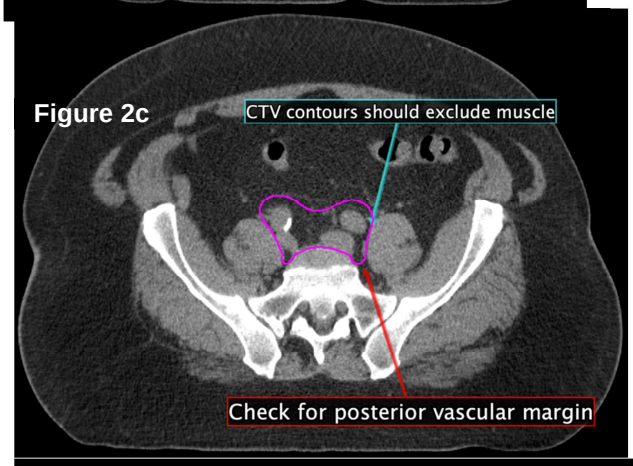
Figure 2c
CTV contours should exclude muscle
Check for posterior vascular margin

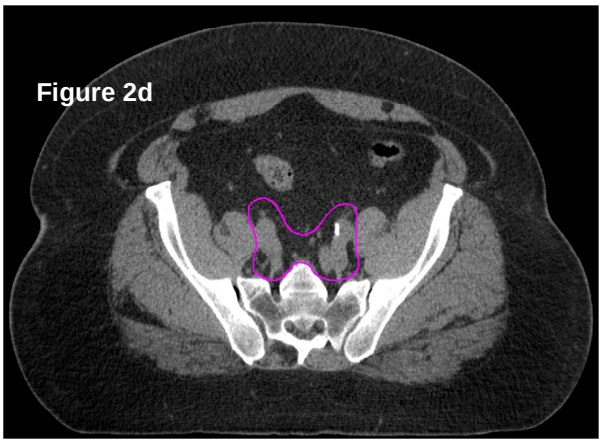
Figure 2d

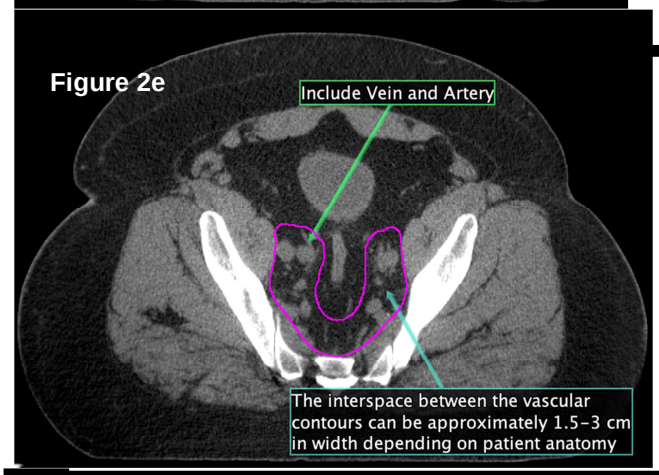
Figure 2e
Include Vein and Artery
The interspace between the vascular contours can be approximately 1.5–3 cm in width depending on patient anatomy

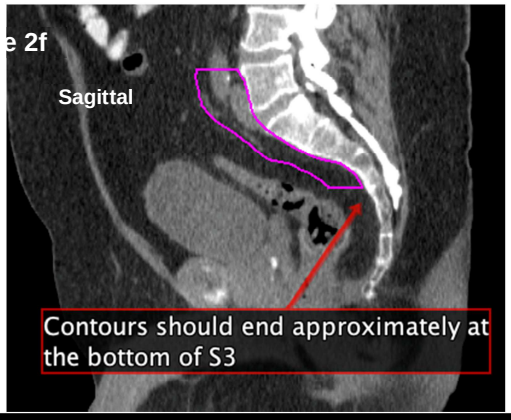
e 2f
Sagittal
Contours should end approximately at the bottom of S3

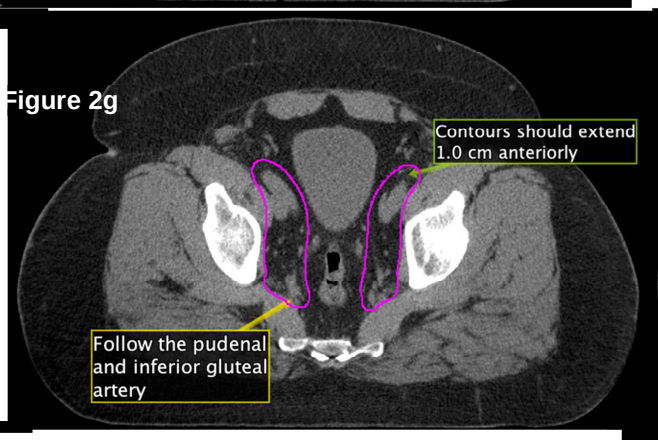
Figure 2g
Contours should extend 1.0 cm anteriorly
Follow the pudenal and inferior gluteal artery

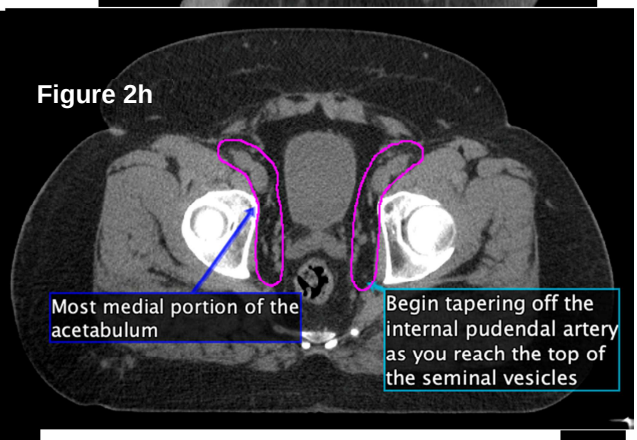
Figure 2h
Most medial portion of the acetabulum
Begin tapering off the internal pudendal artery as you reach the top of the seminal vesicles

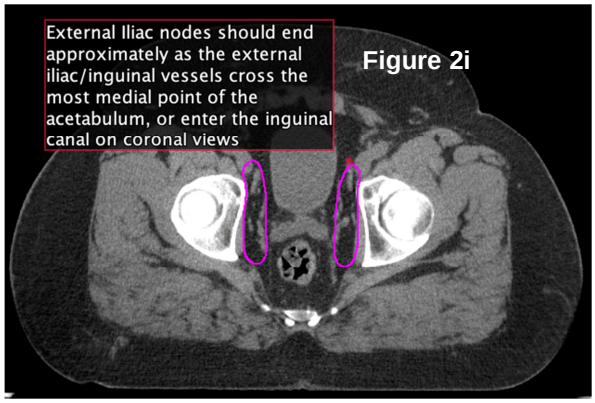
External Iliac nodes should end approximately as the external iliac/inguinal vessels cross the most medial point of the acetabulum, or enter the inguinal canal on coronal views
Figure 2i

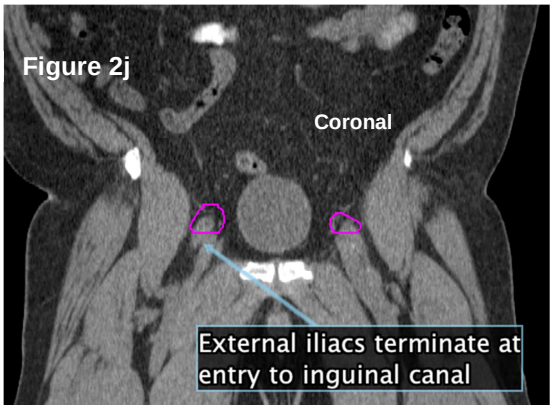
Figure 2j
Coronal
External iliacs terminate at entry to inguinal canal

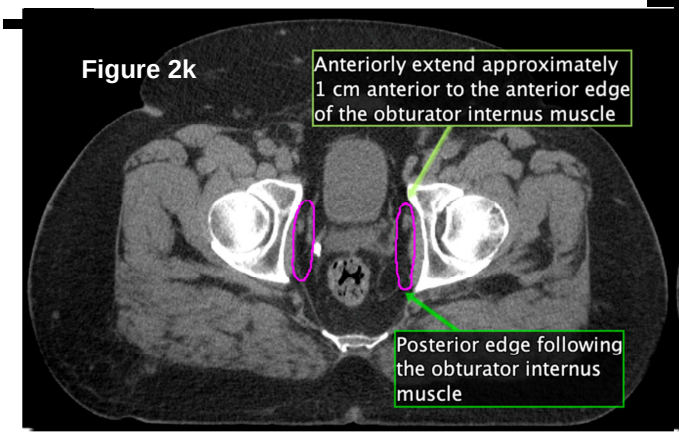
Figure 2k
Anteriorly extend approximately 1 cm anterior to the anterior edge of the obturator internus muscle
Posterior edge following the obturator internus muscle

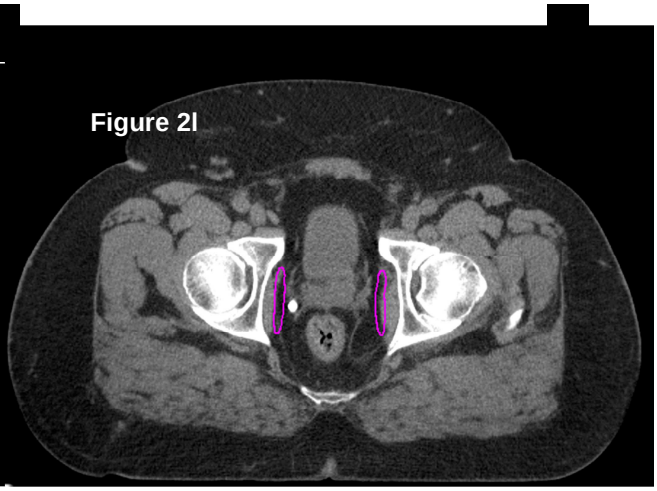
Figure 2l

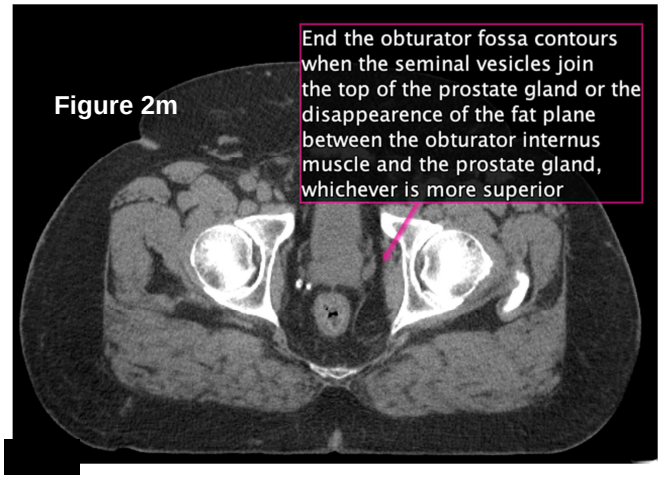
Figure 2m
End the obturator fossa contours when the seminal vesicles join the top of the prostate gland or the disappearence of the fat plane between the obturator internus muscle and the prostate gland, whichever is more superior

Figure 1m

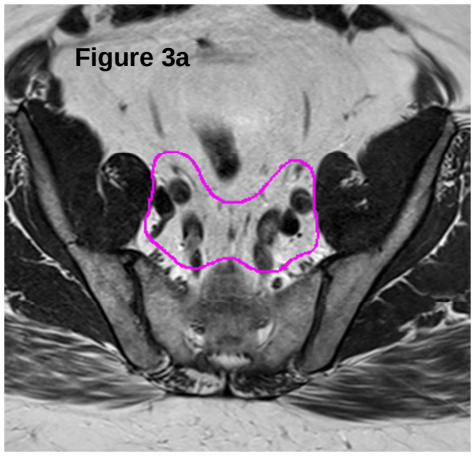
Figure 3a

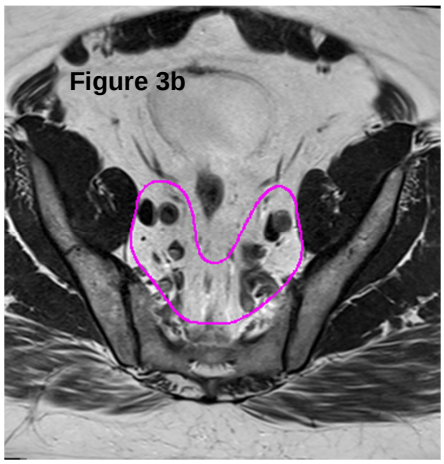
Figure 3b

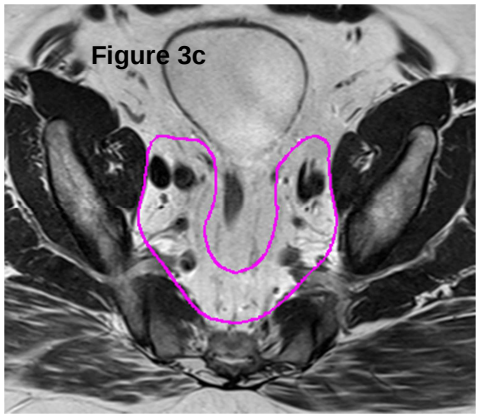
Figure 3c

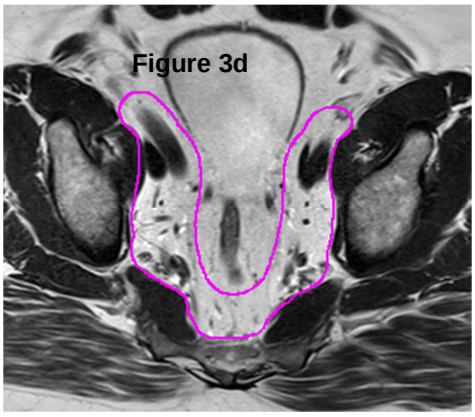
Figure 3d

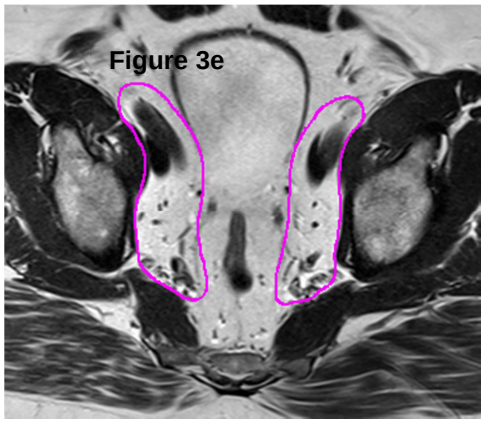
Figure 3e

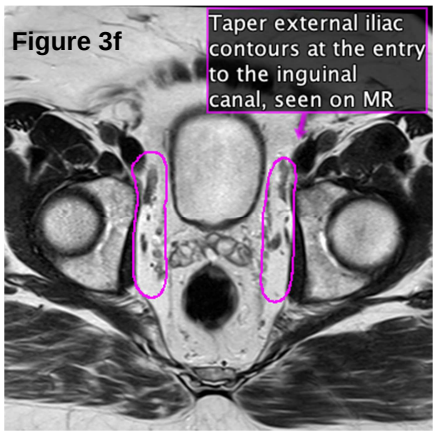
Figure 3f
Taper external iliac contours at the entry to the inguinal canal, seen on MR

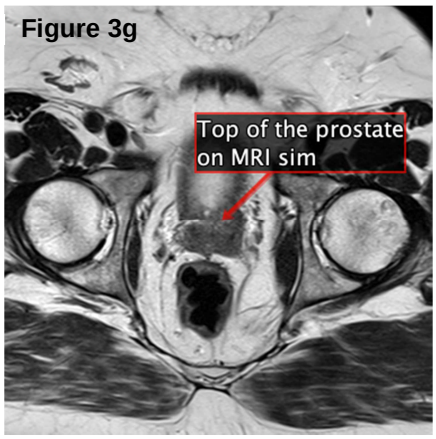
Figure 3g
Top of the prostate on MRI sim